Patterning protein concentration using laser-assisted adsorption by photobleaching, LAPAP†

Jonathan M. Bélisle,[ab] James P. Correia,[c] Paul W. Wiseman,[d] Timothy E. Kennedy[c] and Santiago Costantino*[abe]

Received 11th August 2008, Accepted 3rd October 2008
First published as an Advance Article on the web 17th October 2008
DOI: 10.1039/b813897d

The study of cellular responses to changes in the spatial distribution of molecules in development, immunology and cancer, requires reliable methods to reproduce *in vitro* the precise distributions of proteins found *in vivo*. Here we present a straightforward method for generating substrate-bound protein patterns which has the simplicity required to be implemented in typical life science laboratories. The method exploits photobleaching of fluorescently tagged molecules to generate patterns and concentration gradients of protein with sub-micron spatial resolution. We provide an extensive characterization of the technique and demonstrate, as proof of principle, axon guidance by gradients of substrate-bound laminin peptide generated *in vitro* using LAPAP.

Microfabrication techniques are increasingly being applied to refine cell culture methods in order to precisely reproduce *in vitro*, the spatial distributions of proteins found *in vivo* during key events in development.[1] Nevertheless, the technical challenges of fabricating effective biomimetic protein patterns using existing methods have restricted the use of these new technologies. Here we report a relatively simple technique to tailor arbitrary protein patterns at subcellular resolution that can be implemented using readily available reagents and equipment typically used in life science research labs.

Precise distributions of extracellular proteins are crucial for cellular responses in a myriad of processes that include migration, differentiation and ultimately tissue organization.[2–5] During neural development, axonal growth cones extend and retract filopodia and lamellipodia to determine the path and speed of process extension in order to appropriately wire the nervous system. Several families of guidance cues including netrins, semaphorins, slits and ephrins have now been identified. These bind to specific receptors presented by axonal growth cones which trigger signal transduction pathways that direct cytoskeletal remodeling.[6,7] Neuronal responses to these guidance cues are being investigated biochemically; however, many of the precise details of the pathfinding mechanisms remain elusive, in part due to the lack of adequate *in vitro* assays to mimic the responses made by growth cones *in vivo*.

Several methods have been used to investigate protein gradient function *in vitro*. Passive procedures include Boyden, Zigmond and Dunn chambers, however limitations of all these methods are their inability to maintain a stable gradient over periods of several hours to days and major limitations in their capacity to tailor gradients with specific spatial profiles. The simplicity of generating gradients puffed from a micropipette has made them a convenient tool to study axon guidance,[8,9] but the concentration and shape of gradients produced with this assay have shown important instabilities.[10] Other methods to mimic gradients of membrane or extracellular matrix proteins to study axon guidance were limited in their capacity to reproduce the small scale and steepness of gradients present *in vivo*.[11,12] In addition, the deposition of nanodrops of protein solution[13] and several microfluidic devices[14,15] have also been successfully used to produce gradients, however the requirement for specialized equipment has restricted the use of these methods in subsequent biological studies. Recently, gradients of ephrinA5 were fabricated by soft lithography, changing protein spot densities to influence axon extension of retinal neurons.[16] While this method provides precise and reproducible graded patterns at a macroscopic scale across a few tens of micrometers, it is limited by the fact that the concentration of protein present in each spot remains constant across the entire gradient, and the distribution is only graded in terms of spot size and density. Finally, gradients can also be obtained by varying nanoparticle spacing on a substrate *via* self-assembly of micelles[17] or using a miniature squeegee.[18]

Photonic techniques offer an alternative,[19,20] but generally require the use of UV-lasers and specific chemical cross-linkers that are not commercially available. By contrast, in the approach we describe here, fluorescently tagged molecules are bound to glass substrates by photobleaching the dye molecules. Previous reports of this phenomenon used Hg lamps and large scale photomasks to covalently bind biotin-4-fluorescein (B4F) to BSA adsorbed on a glass surface and thereby generate patterns of substrate-bound protein.[21] Biotin binds to BSA *via* the generation of free radicals after fluorescein photobleaching and this mechanism was tested by varying the oxygen concentration of the buffer solution.[21] However, like the soft-lithography approach,[16] the concentration of substrate-bound protein remained constant within the patterned surfaces.

For the approach we have developed here, laser assisted protein adsorption by photobleaching (LAPAP), B4F is adsorbed to a BSA coated glass substrate using a visible Argon or diode laser and is used as a scaffold to bind protein, and potentially multiple different proteins. In this first step of the protocol, custom patterns of substrate

[a]*Maisonneuve-Rosemont Hospital, University of Montreal, QC, Canada. E-mail: santiago.costantino@umontreal.ca*
[b]*Institute of Biomedical Engineering, University of Montreal, QC, Canada*
[c]*Montreal Neurological Institute, Department of Neurology and Neurosurgery, McGill University, QC, Canada*
[d]*Departments of Physics and Chemistry, McGill University, QC, Canada*
[e]*Department of Ophthalmology, University of Montreal, QC, Canada*

† Electronic supplementary information (ESI) available: Concentration of substrate-bound protein (Streptavidin-Cy5) as a function of both laser power and dwell time (Fig. S1). See DOI: 10.1039/b813897d

bound biotin are produced by moving the focal spot of the laser with respect to the surface. Moreover, since the intensity of the laser illumination regulates the amount of proteins bound to the substrate, the concentration of protein deposited on cell culture substrates can be controlled. The spatial resolution of the technique is determined by the diffraction limit size of the laser focus and the precision of the motorized translation stage. The macroscopic size of the overall pattern is only limited by the size of the surface to be patterned and the range of the motorized microscope stage. The final density of protein linked to the substrate is determined by the total amount of energy applied during photobleaching. Therefore, the scanning velocity, the solution concentration and the intensity of the laser regulate the dynamic range of the amount of proteins that can be linked to the substrates.

Typically, after the laser-adsorption of B4F, the second step is to incubate streptavidin on the sample, which binds to the patterned biotin. For the final step, multiple options are available: either biotinylated peptides or a set of biotinylated antibodies or proteins can be added to the substrate to produce spatially definite patterns of substrate bound, biologically active protein. The full procedure is depicted in Fig.1.

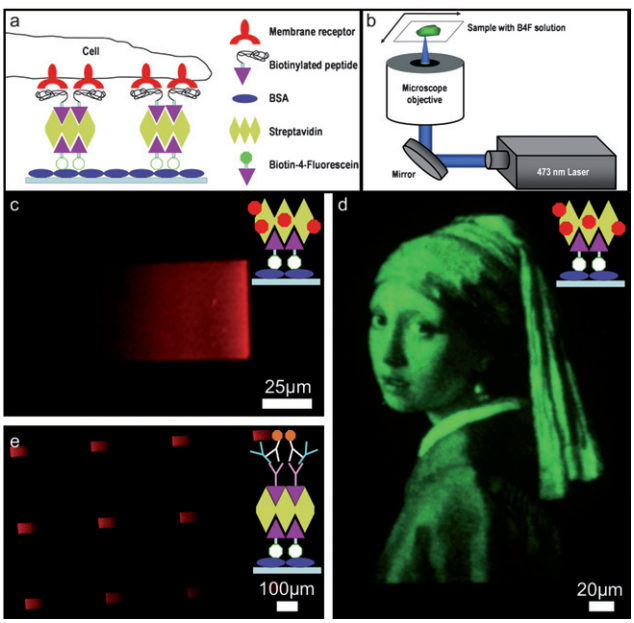

Fig. 1 Examples of protein gradients and patterns obtained by LAPAP and setup. (a) Schematic of the B4F, streptavidin and biotinylated peptide combination required to produce functional protein patterns. B4F is first adsorbed by LAPAP to a BSA-coated substrate, next streptavidin is incubated on the sample and finally a biotinylated peptide is added to produce functional gradients. (b) The simple patterning apparatus includes a blue diode laser, a microscope objective and motorized translation stages to move the sample with respect to the focal spot. (c) Continuous gradient of streptavidin-Cy5 produced by changing both the laser intensity and the velocity of the focal spot displacement. (d) Streptavidin-Cy5 miniature reproduction of Vermeer's Girl With a Pearl Earring that demonstrates the flexibility and dynamic range of the technique. (e) Gradients of rabbit anti-laminin with the same shape as that shown in (c), immunostained using Alexa 594 goat anti-rabbit IgG. To produce and visualize these gradients, B4F was first adsorbed by LAPAP, followed by 4 subsequent incubation steps: streptavidin, biotinylated anti-rabbit IgG, rabbit anti-laminin and Alexa 594 goat anti-rabbit IgG.

The LAPAP setup consisted of a 473 nm diode laser (Laserglow, ON, Canada), a motorized xyz translation stage (Thorlabs, NJ) and a 60x 1.2 NA water immersion objective (Olympus, Japan). The movement of the motorized stage and laser intensity were controlled by a custom-made Labview (National Instrument, TX) program. A solution of 3% bovine serum albumin (BSA) was added for 20 min to minimize non-specific protein adsorption in 10 mm microwell culture dishes (MatTek Corporation, MA). A 40 μL drop of 50 μg/mL of B4F (Anaspec, CA) in 3% BSA was placed on the surface of glass-bottom culture dishes before performing the photobleaching process. The total number of gradients on a culture dish was user-defined and depending on the complexity of shape and slope of the gradient, approximately 30 s to 3 min were required to generate each gradient.

The B4F solution was then rinsed with PBS and then incubated with 5 μg/mL streptavidin-Cy5 (Invitrogen, CA) in 3% BSA solution for 30 min. To produce functional peptide gradients, 5 μg/mL of a biotinylated peptide (CSRARKQAASIKVAVSADR, commonly named IKVAV peptide) in 3% BSA was then incubated on the microwell plate for 25 min. Fig. 1a and Fig. 1b present schematics of gradients obtained using biotinylated peptides and of the patterning setup.

Various examples of protein gradients and patterns fabricated using LAPAP are shown in Fig. 1. Panel 1c illustrates a gradient of streptavidin-Cy5 composed of 100 lines 50 μm in length, spaced by 1 μm. The first 60 lines were made at a constant laser scan velocity of 50 μm/s and increasing laser intensity incrementally from line to line from 0.5 to 160 μW. A constant intensity of 160 μW and a sequentially decreasing line scan velocity (from 49 to 5 μm/s) were used for the final 40 lines.

Additionally, using biotinylated antibodies, patterns of specific antigens can be fabricated. To create full protein gradients (in this case using antibodies against the extracellular matrix protein laminin-1), the peptide incubation step is replaced by three 30 minutes steps of biotinylated anti-rabbit IgG (5 μg/mL), followed by rabbit anti-laminin (5 μg/mL) and then Alexa 594 goat anti-rabbit IgG (20 μg/mL). The first biotinylated antibody is used to link the target protein (rabbit anti-laminin) to the substrate. The fluorescently tagged IgG is then used to visualize the distribution. Fig. 1e illustrates several gradients of rabbit anti-laminin revealed with the Alexa 594 goat anti-rabbit IgG, all created using the same parameters as for the gradient shown in Fig. 1c. Finally, the flexibility and precision of this method to fabricate substrates with a wide dynamic range of adsorbed protein concentration is demonstrated by reproducing a 200 × 293-pixels image of Vermeer's "Girl With a Pearl Earring" (Fig. 1d). Each pixel from the image scales to 1μm^2 on the pattern.

To characterize the dynamic range of LAPAP as a function of laser power, an analysis of photobleaching dwell time compared to B4F concentration was performed. Lines were first scanned at different beam focus velocities from 200 to 2 μm/s and we compared the fluorescence intensity present in different regions of the pattern generated while assuming a linear relationship between fluorescence signal and protein concentration. We applied a simple model where the adsorption rate of B4F is proportional to the available B4F-free surface within the area delimited by the focal spot of the laser. Therefore, the adsorbed protein concentration (θ) as a function of the laser dwell time (t) behaves exponentially: $\theta = \theta_{max}(1\text{-}e^{-t/\tau})$, where θ_{max} is the maximum protein concentration that can be adsorbed and τ is a characteristic time constant. As shown in Fig. 2a, protein

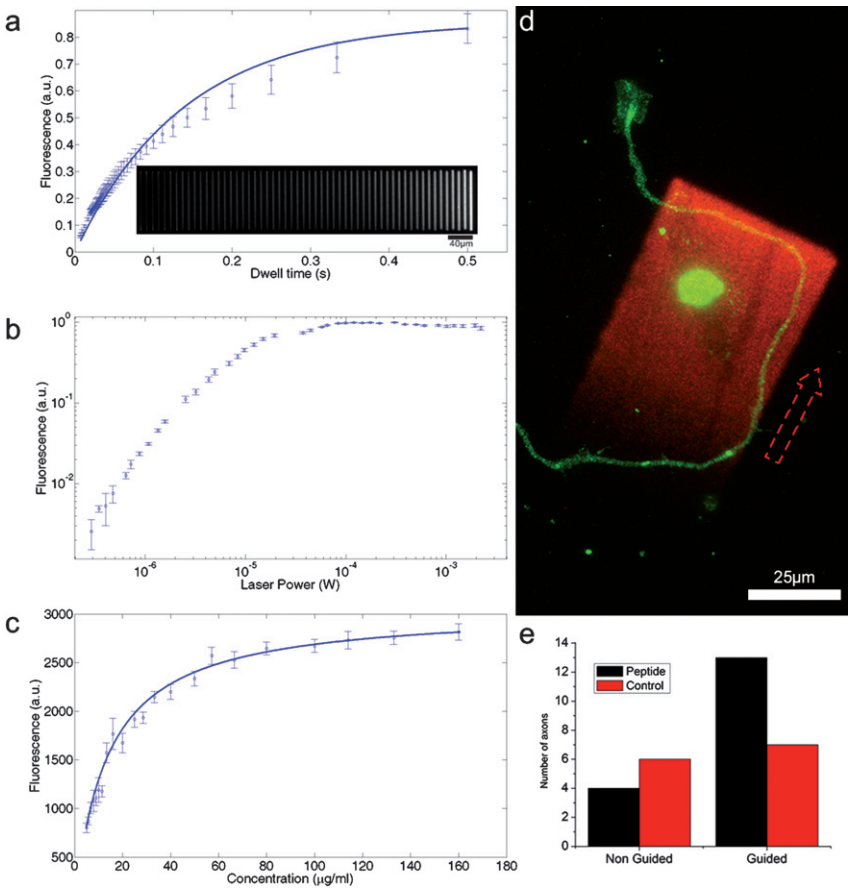

Fig. 2 Characterization of the patterning method and growth cone guidance assay. (a) Adsorbed protein concentration as measured by fluorescence as a function of beam dwell time shows an exponential behavior. The inset shows one of the 10 patterns created to produce this graph. (b) Adjusting the laser power allows the user to modulate the protein concentration range over more than two orders of magnitude. Maximum protein concentration is reached at approximately 160 μW. (c) By varying the concentration of B4F, we show that bound protein concentration follows a Langmuir isotherm. (d) An example of axonal guidance by a gradient of IKVAV peptide. DRG neuron stained with Alexa 546 in green and laminin peptide gradient visualized by streptavidin-Cy5 in red. The red arrow points to the direction of increasing concentration. The green circular spot in the middle of the gradient is debris resulting from tissue dissection. This neuron was scored as guided. (e) Axonal response on laminin peptide gradients and on control samples. Axons were considered "guided" if they traveled along the gradient's positive slope, and "non-guided" when they traveled in the opposite direction.

concentration was well modeled by this function yielding a time constant of 0.14 s.

The amount of substrate bound protein was found to increase with laser power from 1.9 to 160 μW when using a 1.2 NA objective. For laser intensities beyond this threshold a plateau can be observed in protein concentration up to an intensity of 3.1 mW, likely due to photobleaching saturation (Fig 2b). The protein concentration as a function of B4F solution concentration follows a Langmuir isotherm (Fig 2c).

To test the biochemical activity of the peptide gradients generated, dorsal root ganglion (DRG) cells isolated from E15 Sprague Dawley rat embryos were grown on gradients of a laminin fragment that has been previously demonstrated to be sufficient to evoke axonal growth cone turning by these cells[19] (Fig 2d). Dissociated DRG cultures were cultured in neurobasal supplemented with 2% B-27, 2 mM GlutaMAX-1, 100 unit/mL penicillin, 100 μg/mL streptomycin, and 50 ng/mL NGF. Before LAPAP, the substrates were coated with poly-D-Lysine (2 μg/mL) for 10 min to promote attachment of the neurons to the coverglass. DRG cells were grown on IKVAV gradients and also on control samples where the laminin peptide was replaced by B4F (5 μg/mL). After 24 to 36 hours, the cultures were fixed in 4% paraformaldehyde and neurons were immunostained using 0.8 unit/mL Alexa 546 coupled phalloidin and 500 ng/mL Hoechst 33258.

In order to quantify the behavior of growth cones on the peptide patterns, the samples were imaged using fluorescence microscopy and analyzed. Axons were counted as "guided" if they entered the patterned area and traveled up the gradient, and as "non-guided" if they traveled down the gradient before exiting the pattern. The images were randomly numbered and analyzed by an observer blind to the experimental conditions, i.e. unaware if the sample substrate consisted of IKVAV peptide or were controls (Fig. 2e). The number of axons extending in the positive direction on the IKVAV gradient was three times greater than the number turning in the opposite direction. On control substrate, axons showed no preferential direction. Fig. 2d illustrates an example of an axon that was scored as turning and extending up a gradient of the IKVAV peptide. Fig. 2e shows the cumulative results of a total of 400 gradients (200 controls and 200 IKVAV peptides), on which 30 axons were identified and scored as having encountered a gradient, independent of interactions with other cells. Both continuous gradients as in Fig. 1c (400 in total)

and gradients composed of separated lines (694) to reduce fabrication time were patterned. Line gradients consist of 11 lines of a 100 μm length spaced by 10 μm with a measured thickness of 1.26 ± 0.07 μm. A six-fold reduction in the fabrication time of the discrete gradients allowed doubling of the covered area as compared to continuous gradients. The guiding capacity of each type of gradient, continuous and spaced, was quantified independently and no guidance observed on the striped pattern for 131 growth cones. In addition, the total number found on the peptide patterns doubled the number of those on control samples (considering the 1094 patterns).

As compared to conventional assays, LAPAP can create protein patterns that have a resolution close to one micron (1.26 ± 0.07 μm for the 1.2 NA objective used), their spatial distribution is arbitrary and their full size is only limited by the range of travel of the stage used. The simplicity of LAPAP allows for straightforward implementation on a motorized confocal microscope, with only software customizations. Moreover, the fact that laser light does not interact with the final protein patterned, eliminates the chances of protein photodamage as compared to other photonic techniques.[19] Fabricated gradients remain stable over extended periods of time as we have found that they can still be visualized after more than three months of storage at 4 °C. Finally, by varying beam dwell time and solution concentration, it is possible to change the amount of protein bound by an order of magnitude for each parameter (Fig. 2a and c). Manipulation of the laser power provides additional control, readily providing the ability to vary the fluorescence from the bound protein by over two orders of magnitude (Fig. 2b). By combining adjustments of the laser power and dwell time we show that the range of bound protein can be extended by three orders of magnitude (ESI Fig. S1†). Furthermore, minimizing non-specific binding of proteins to the substrate could further increase this range.

The studies presented demonstrate the versatility and potential of this simple approach. Nevertheless, chemotaxis in a living organism implies complex distributions of a plethora of guidance cues and to understand and manipulate this requires a means to generate more complex protein distributions and combinations. Our current studies aim to extend LAPAP to link more than one guidance cue by increasing the number of fluorescent tags and laser lines, and additionally to carrying out functional chemotaxis assays using full-length proteins.

In conclusion, we report a novel assay for precise and flexible generation of protein distributions on cell culture substrates. LAPAP provides a relatively straight forward method that allows the generation of graded distributions of substrate bound protein at subcellular levels of resolution.

Acknowledgements

Support is acknowledged for SC from the NSERC and FQRNT, for PWW from NSERC and CIHR, for TEK from FRSQ and CIHR, and for JMB from NSERC (CGS D). We acknowledge Simon W. Moore for helpful discussion during the beginning of this project. PWW and TEK acknowledge the support of the CIHR funded program in neuroengineering for this work.

Notes and references

1 T. M. Keenan and A. Folch, *Lab Chip*, 2008, **8**, 34–57.
2 T. E. Kennedy, H. Wang, W. Marshall and M. Tessier-Lavigne, *J. Neurosci.*, 2006, **26**, 8866–8874.
3 M. Tessier-Lavigne and C. S. Goodman, *Science*, 1996, **274**, 1123–1133.
4 H. L. Ashe and J. Briscoe, *Development*, 2006, **133**, 385–394.
5 C. A. Parent and P. N. Devreotes, *Science*, 1999, **284**, 765–770.
6 B. J. Dickson, *Science*, 2002, **298**, 1959–1964.
7 J. K. Chilton, *Dev. Biol.*, 2006, **292**, 13–24.
8 R. W. Gundersen and J. N. Barrett, *Science*, 1979, **206**, 1079–1080.
9 J. Q. Zheng, M. Felder, J. A. Connor and M. M. Poo, *Nature*, 1994, **368**, 140–144.
10 Z. Pujic, C. E. Giacomantonio, D. Unni, W. J. Rosoff and G. J. Goodhill, *J. Neurosci. Methods*, 2008, **170**, 220–228.
11 M. P. McKenna and J. A. Raper, *Dev. Biol.*, 1988, **130**, 232–236.
12 H. Baier and F. Bonhoeffer, *Science*, 1992, **255**, 472–475.
13 W. J. Rosoff, J. S. Urbach, M. A. Esrick, R. G. McAllister, L. J. Richards and G. J. Goodhill, *Nat. Neurosci.*, 2004, **7**, 678–682.
14 B. G. Chung, F. Lin and N. L. Jeon, *Lab Chip*, 2006, **6**, 764–768.
15 S. K. Dertinger, X. Jiang, Z. Li, V. N. Murthy and G. M. Whitesides, *Proc. Natl. Acad. Sci. USA*, 2002, **99**, 12542–12547.
16 A. C. von Philipsborn, S. Lang, J. Loeschinger, A. Bernard, C. David, D. Lehnert, F. Bonhoeffer and M. Bastmeyer, *Development*, 2006, **133**, 2487–2495.
17 M. Arnold, V. C. Hirschfeld-Warneken, T. Lohmuller, P. Heil, J. Blummel, E. A. Cavalcanti-Adam, M. Lopez-Garcia, P. Walther, H. Kessler, B. Geiger and J. P. Spatz, *Nano Lett.*, 2008, **8**, 2063–2069.
18 S. Costantino, C. G. McQuinn, T. E. Kennedy and P. W. Wiseman, *J. Biochem. Biophys. Methods*, 2008, **70**, 1192–1195.
19 D. N. Adams, E. Y. Kao, C. L. Hypolite, M. D. Distefano, W. S. Hu and P. C. Letourneau, *J. Neurobiol.*, 2005, **62**, 134–147.
20 A. Buxboim, M. Bar-Dagan, V. Frydman, D. Zbaida, M. Morpurgo and R. Bar-Ziv, *Small*, 2007, **3**, 500–510.
21 M. A. Holden and P. S. Cremer, *J. Am. Chem. Soc.*, 2003, **125**, 8074–8075.